Sensors and Materials, Vol. 36, No. 2 (2024) 499–506
MYU Tokyo

S & M 3537

Photoluminescence and Radioluminescence Properties of $Y_3Al_5O_{12}$ Doped with 3d-transition Metal Ions

Noriaki Kawaguchi,[1*] Naoki Hayashi,[2] Toshiaki Kunikata,[1] Kensei Ichiba,[1] Takumi Kato,[1] Daisuke Nakauchi,[1] and Takayuki Yanagida[1]

[1]Nara Institute of Science and Technology, 8916-5 Takayama, Ikoma, Nara 630-0192, Japan
[2]Yamato University, 2-5-1 Katayama-cho, Suita-shi, Osaka 564-0082, Japan

(Received November 5, 2023; accepted January 18, 2024)

Keywords: scintillator, 3d-transition metal ions, single crystal

The photoluminescence and radioluminescence properties of $Y_3(Al_{0.99}TM_{0.01})_5O_{12}$ (*TM* = Ti, V, Mn, and Cu) single crystals were investigated. Single crystalline rods of approximately 5 mm diameter were grown by the optical floating zone method. The photoluminescence quantum yields of the obtained single crystals were 1.3–3.8%. Both the intrinsic luminescence of $Y_3Al_5O_{12}$ (YAG) and the extrinsic luminescence due to each dopant were observed in the radioluminescence spectra. The radioluminescence decay times of YAG doped with either Ti, V, Mn, or Cu were in the range from 6.9 μs to 10.2 ms.

1. Introduction

Sensing techniques, such as radiation detection,[1] bio-imaging,[2] and thermometry,[3] are some of the applications of luminescent materials. In particular, luminescent materials for radiation detection, which emit light under radiation excitation and are called scintillators, have many applications including medical, industrial, and scientific ones. Although many scintillators have been studied in the last few decades,[4–7] fundamental studies on novel scintillators still continue to achieve better performance than ever before. There have been reports on various types of scintillator, such as single crystals,[8–21] nanocrystals,[22] crystalline films,[23] ceramics,[24–27] glasses,[28–37] plastics,[38] and organic–inorganic hybrid materials,[39–42] even in the last few years. In terms of the luminescent center, specific dopants such as Ce, Eu, and Tl have been mainly used for commercial scintillators; however, other dopants are also of our interest.

In this study, we investigated the photoluminescence (PL) and radioluminescence (RL) properties of $Y_3Al_5O_{12}$ (YAG) doped with 3d-transition metal ions. We chose Ti, V, Mn, and Cu as 3d-transiton metals because they have been known or studied as dopants of luminescent materials for laser lighting and displays, such as Ti-doped Al_2O_3,[43] V-doped YAG,[44] Mn-doped ZnS,[45] and Cu-doped glasses.[46,47] Since garnet-type single crystals

*Corresponding author: e-mail: n-kawaguchi@ms.naist.jp
https://doi.org/10.18494/SAM4768

ISSN 0914-4935
https://myukk.org/

have been one of the most well-known host crystals for scintillators, we chose YAG as the host crystal.

2. Materials and Methods

$Y_3(Al_{0.99}TM_{0.01})_5O_{12}$ (*TM* = Ti, V, Mn, and Cu) single crystals were grown by the optical floating zone (FZ) method. Because the ionic radii of the dopants were closer to that of Al than to that of Y, we expected that dopants would replace Al. Raw powders of Y_2O_3 (4N; Furuuchi Chemical), Al_2O_3 (4N; Kojundo Chemical Laboratory), TiO_2 (4N; Kojundo Chemical Laboratory), V_2O_5 (4N; Kojundo Chemical Laboratory), MnO (3N; Furuuchi Chemical), and Cu_2O (2N; Kojundo Chemical Laboratory) were mixed and ground using an agate mortar and pestle. Each mixed powder was shaped into a rod by hydrostatic pressure and sintered at 1400 °C for 8 h in air. The sintered rods were crystallized using an optical FZ furnace (FZD0192; Canon Machinery). Each rod was rotated at 7 rpm and partially melted using two halogen lamps facing each other. The melted zone moved gradually at 3 mm/h. All the obtained single crystals were confirmed to be single phases of YAG by X-ray diffraction analysis.

PL quantum yields (*QY*s) and excitation-emission maps were measured using a PL spectrometer (Quantaurus-QY; Hamamatsu Photonics). PL decay curves were recorded using Quantaurus-τ C11367 (Hamamatsu Photonics). The obtained PL decay curves were fitted with exponential functions to estimate decay times. RL spectra were measured using our customized measurement system.[48] RL decay curves were measured using our other customized measurement system[49] and analyzed in the same manner as PL.

3. Results and Discussion

Figure 1 shows the PL excitation–emission maps, PL decay curves, and appearances of YAG single crystals doped with either Ti, V, Mn, or Cu. The obtained YAG samples were transparent, and no inclusions were found in them by visual observation. In addition, the Ti-, V-, Mn-, and Cu-doped YAG samples looked colorless, green, red, and light brown, respectively. Differences in the colors of the samples might be caused by the absorption of each dopant. The maximum PL *QY*s of Ti-, V-, Mn-, and Cu-doped YAG samples were 1.3, 3.6, 3.8, and 3.7%, respectively. The PL *QY*s of the samples were low; however, they might increase if the dopant concentration is optimized.

Two emission peaks at around 470 and ~790 nm were observed in the PL excitation–emission map of the Ti-doped YAG sample upon 280 nm excitation. The PL decay times of the Ti-doped YAG sample at around 470 and ~790 nm were estimated to be approximately 31.5 μs and 8.0 ms, respectively. The emission peak at around 470 nm would be attributed to the charge transfer (CT) transition of Ti^{4+} ions.[50,51] Various decay times of this emission have been reported, for example, that of Ti, Si-doped Al_2O_3 has been reported to be 42.9 μs,[52] which was roughly consistent with that of the Ti-doped YAG sample. Ti-doped materials can show luminescence in the red wavelength region owing to the d–d transitions of Ti^{3+} ions.[53,54] This is not an origin of the emission of our Ti-doped YAG sample at ~790 nm since the decay time is significantly

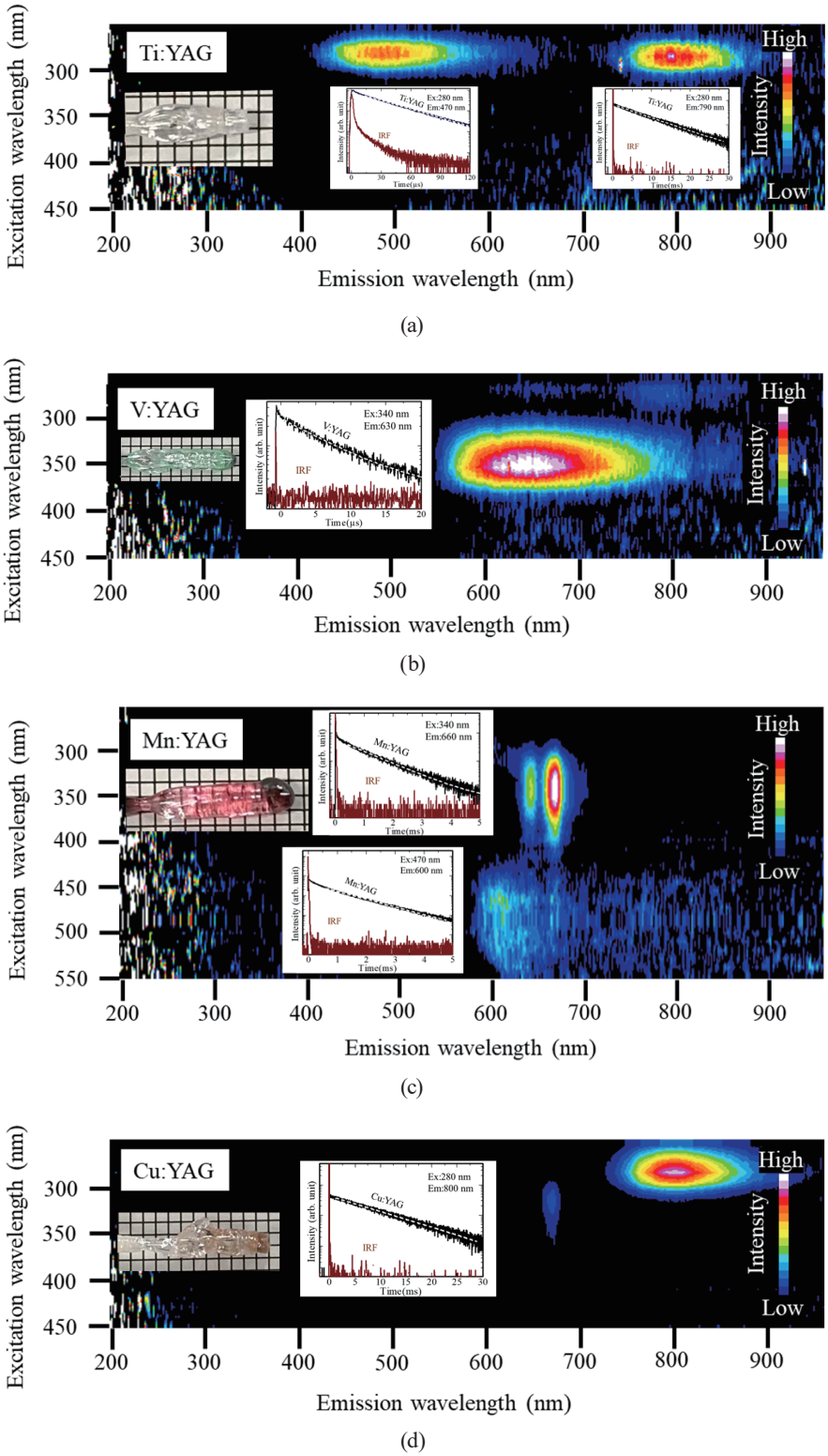

Fig. 1. (Color online) From top to bottom, PL excitation–emission maps, PL decay curves, and appearances of YAG single crystals doped with either (a) Ti, (b) V, (c) Mn, or (d) Cu.

different. For example, the decay time of the d-d luminescence of Ti-doped Al_2O_3 is 3.2 μs,[43] whereas that of our sample is approximately 8.0 ms. The origin of the emission at ~790 nm could be explained by the $^4T_1$–$^6A_1$ transition of Fe^{3+} ions,[55–58] which was an unexpected contaminant.

In the case of V-doped YAG, one emission peak at 630 nm was observed and its excitation peak wavelength was ~ 340 nm. The decay curve of the V-doped YAG sample was approximated by a single exponential function and its decay time was ~6.9 μs. A possible origin of this emission is the CT transition between V^{5+} and O^{2-}, which can show decay times of a few μs. This CT emission has various excitation and emission wavelengths, which change depending on the V–O distance.[59] For example, the excitation and emission wavelengths of $VAlO_4$ are around 330–360 and 620 nm, respectively,[60] which are consistent with those of the V-doped YAG sample. In a previous study, the excitation and emission wavelengths of the CT emission of V-doped YAG were reported to be 266 and 570 nm, respectively.[44] The reason for the slightly different wavelengths may be due to the difference in the sensitivities of the detectors.

Three emission peaks at around 600, 640, and 660 nm were observed in the Mn-doped YAG, and excitation peak wavelengths were at around 470, 340, and 340 nm, respectively. The decay curves of emissions at 600 and 640–660 nm were successfully fitted by a single exponential function, and their decay times were estimated to be approximately 1.1 and 1.0 ms, respectively. Results were consistent with the previous report on Mn-doped YAG.[61] The emission at 600 nm was ascribed to the $^4T_1$–$^6A_1$ transitions of Mn^{2+} ions, and the emissions at 640 and 660 nm were ascribed to the $^4T_2$–$^4A_2$ transitions of Mn^{4+} ions.

The Cu-doped YAG sample showed an emission peak at ~800 nm and weak emissions at 640–660 nm. The decay time at 800 nm was ~8.6 ms. The decay curve of the weak emissions at 640–660 nm was not clearly observed because of the low emission intensity. These emissions were not consistent with those originating from the Cu dopant. Possible origins would be the unexpected impurities containing Fe^{3+} and Mn^{2+} ions. The emission at ~800 nm was consistent with that due to the $^4T_1$–$^6A_1$ transition of Fe^{3+} ions.[55,56] The emission due to Fe^{3+} contamination was observed also in the Ti-doped YAG sample. Unfortunately, our single crystals seemed to be easily contaminated by Fe^{3+} ions because we often used iron oxide powders, which were put on raw material rods as a light absorber in heating during the crystal growth using the optical FZ furnace. The weak emission at 640–660 nm was consistent with those due to the $^4T_2$–$^4A_2$ transitions of Mn^{4+} ions.[61] The Mn^{4+} ions seem to be present in the Cu-doped YAG single crystal as contamination. Because the Mn-doped YAG single crystal was also prepared, the Cu-doped YAG sample could be contaminated by Mn^{4+} ions from experimental apparatus for sample preparation.

Figure 2 shows the X-ray-excited RL spectra and RL decay curves of the Ti-, V-, Mn-, and Cu-doped YAG samples. In the RL spectra of all the samples, emission in a broad wavelength range from 300 to 400 nm was observed. This is the significant difference between PL and RL. These broad emissions can be ascribed to the intrinsic luminescence of YAG owing to defect-related transitions[62] or self-trapped excitons.[63] Most of the emission peaks in the PL spectra were observed also in the RL; however, the emission peaks of the Ti- and Cu-doped YAG samples at ~800 nm were not detected even when using a red-sensitive CCD. The emission peak

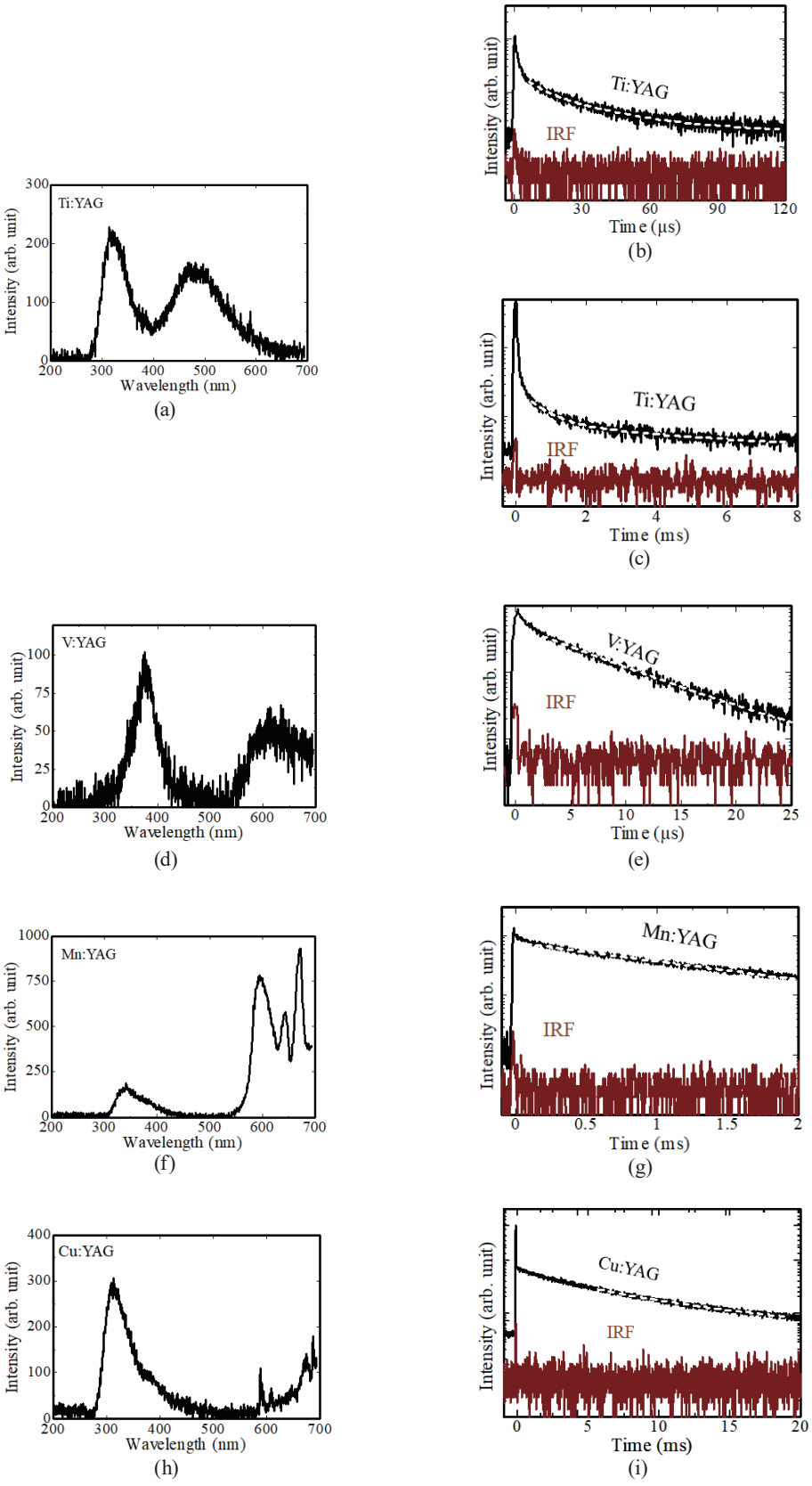

Fig. 2. (Color online) RL spectra of YAG single crystals doped with (a) Ti, (d) V, (f) Mn, or (h) Cu. Their RL decay curves are also shown in (b), (c), (e), (g), and (i).

of the Cu-doped YAG at around 640–660 nm was also not detected owing to the low emission intensity of impurity Mn^{4+} ions.

The RL decay curves of the Ti-doped YAG were measured with two time ranges, and each decay curve was approximated with a double exponential function. The RL decay curves of the V-, Mn-, and Cu-doped YAG were approximated by single exponential functions. The RL decay times of the Ti-doped YAG sample were estimated to be 8.5 and 32.8 μs for the 400 μs range measurement and 0.5 and 4.1 ms for the 50 ms range measurement. The RL decay times of the V-, Mn-, and Cu-doped YAG were estimated to be 6.9 μs, 1.3 ms, and 10.2 ms, respectively. The estimated values are roughly consistent with those of the PL decay times. Since the wavelength was not resolved in the RL decay measurements, multiple emission components were included, and some of the RL decay curves were not approximated by a single exponential function but a double exponential one. However, no intrinsic luminescence of YAG was detected in the RL decay curve measurements because we used a photomultiplier tube (PMT) that is sensitive in the visible to red region. The obtained RL decay times were in the range from 6.9 μs to 10.2 ms.

4. Conclusions

The PL and RL properties of V-, Mn-, and Cu-doped YAG single crystals were studied. Emission peaks were ascribed to the intrinsic luminescence of YAG or the extrinsic luminescence due to dopants or unexpected impurity ions. The RL decay times of the samples were in the range from 6.9 μs to 10.2 ms. Since the RL decay time of the V-doped YAG sample was relatively short, it might be used in photon-counting radiation detectors. Other samples might be used for radiation detectors that are operated in the current mode.

Acknowledgments

This work was supported by Grants-in-Aid for Scientific Research A (22H00309), Scientific Research B (22H03872, 22H02939, 21H03733, and 21H03736), and Challenging Exploratory Research (22K18997) from the Japan Society for the Promotion of Science. The Cooperative Research Project of the Research Center for Biomedical Engineering, A-STEP (JPMJTM22DN) from JST, Konica Minolta Science and Technology Foundation, Nakatani Foundation, and Kazuchika Okura Memorial Foundation are also acknowledged.

References

1 G. F. Knoll: Radiation Detection and Measurement (Wiley, New York, 2010) 4th ed.
2 J. H. S. K. Monteiro: Molecules **25** (2020) 2089. https://doi.org/10.3390/molecules25092089
3 C. D. S. Brites, R. Marin, M. Suta, A. N. Carneiro Neto, E. Ximendes, D. Jaque, and L. D. Carlos: Adv. Mater. **35** (2023) 2302749. https://doi.org/10.1002/adma.202302749
4 C. W. E. van Eijk: Nucl. Instrum. Methods Phys. Res., Sect. A **460** (2001) 1. https://doi.org/10.1016/S0168-9002(00)01088-3
5 S. E. Derenzo, M. J. Weber, E. Bourret-Courchesne, and M. K. Klintenberg: Nucl. Instrum. Methods Phys. Res., Sect. A **505** (2003) 111. https://doi.org/10.1016/S0168-9002(03)01031-3
6 C. W. E. van Eijk, A. Bessière, and P. Dorenbos: Nucl. Instrum. Methods Phys. Res., Sect. A **529** (2004) 260. https://doi.org/10.1016/j.nima.2004.04.163

7 T. Yanagida, T. Kato, D. Nakauchi, and N. Kawaguchi: Jpn. J. Appl. Phys. **62** (2023) 010508. https://doi.org/10.35848/1347-4065/ac9026
8 H. Fukushima, D. Nakauchi, T. Kato, N. Kawaguchi, and T. Yanagida: Jpn. J. Appl. Phys. **62** (2023) 010506. https://doi.org/10.35848/1347-4065/ac9105
9 D. Nakauchi, T. Kato, N. Kawaguchi, and T. Yanagida: Jpn. J. Appl. Phys. **62** (2023) 010607. https://doi.org/10.35848/1347-4065/ac9181
10 Y. Fujimoto and K. Asai: Jpn. J. Appl. Phys. 62, **010605** (2023). https://doi.org/10.35848/1347-4065/ac9348
11 N. Kawaguchi, T. Kato, D. Nakauchi, and T. Yanagida: Jpn. J. Appl. Phys. **62** (2023) 010611. https://doi.org/10.35848/1347-4065/ac99c3
12 D. Yuan, E. G Víllora, N. Kawaguchi, D. Nakauchi, T. Kato, T. Yanagida, and K. Shimamura: Jpn. J. Appl. Phys. **62** (2023) 010614. https://doi.org/10.35848/1347-4065/aca3e5
13 H. Fukushima, D. Nakauchi, T. Kato, N. Kawaguchi, and T. Yanagida: Sens. Mater. **35** (2023) 429. https://doi.org/10.18494/SAM4139
14 D. Shiratori, H. Fukushima, D. Nakauchi, T. Kato, N. Kawaguchi, and T. Yanagida: Sens. Mater. **35** (2023) 439. https://doi.org/10.18494/SAM4140
15 P. Kantuptim, T. Kato, D. Nakauchi, T. Kato, N. Kawaguchi, K. Watanabe, and T. Yanagida: Sens. Mater. **35** (2023) 451. https://doi.org/10.18494/SAM4141
16 K. Okazaki, D. Nakauchi, H. Fukushima, T. Kato, N. Kawaguchi, and T. Yanagida: Sens. Mater. **35** (2023) 459. https://doi.org/10.18494/SAM4144
17 Y. Fujimoto, D. Nakauchi, T. Yanagida, M. Koshimizu, and K. Asai: Sens. Mater. **34** (2022) 629. https://doi.org/10.18494/SAM3693
18 T. Yanagida, T. Kato, D. Nakauchi, and N. Kawaguchi: Sens. Mater. **34** (2022) 595. https://doi.org/10.18494/SAM3684
19 D. Nakauchi, H. Fukushima, T. Kato, N. Kawaguchi, and T. Yanagida: Sens. Mater. **34** (2022) 611. https://doi.org/10.18494/SAM3696
20 M. Akatsuka, D. Nakauchi, T. Kato, N. Kawaguchi, and T. Yanagida: Sens. Mater. **34** (2022) 619. https://doi.org/10.18494/SAM3692
21 P. Kantuptim, D. Nakauchi, T. Kato, N. Kawaguchi, and T. Yanagida: Sens. Mater. **34** (2022) 603. https://doi.org/10.18494/SAM3690
22 M. Koshimizu, Y. Fujimoto, and K. Asai: Sens. Mater. **35** (2023) 521. https://doi.org/10.18494/SAM4149
23 A. Ito and S. Matsumoto: Jpn. J. Appl. Phys. **62** (2023) 010612. https://doi.org/10.35848/1347-4065/aca249
24 Y. Shao, R. L. Conner, N. R. S. Souza, R. S. Silva, and L. G. Jacobsohn: Jpn. J. Appl. Phys. **62** (2023) 010601. https://doi.org/10.35848/1347-4065/ac9941
25 D. Nakauchi, F. Nakamura, T. Kato, N. Kawaguchi, and T. Yanagida: Sens. Mater. **35** (2023) 467. https://doi.org/10.18494/SAM4138
26 T. Kunikata, T. Kato, D. Shiratori, P. Kantuptim, D. Nakauchi, N. Kawaguchi, and T. Yanagida: Sens. Mater. **35** (2023) 491. https://doi.org/10.18494/SAM4145
27 T. Kunikata, T. Kato, D. Shiratori, D. Nakauchi, N. Kawaguchi, and T. Yanagida: Sens. Mater. **34** (2022) 661. https://doi.org/10.18494/SAM3683
28 K. Shinozaki, G. Okada, N. Kawaguchi, and T. Yanagida: Jpn. J. Appl. Phys. **62** (2023) 010603. https://doi.org/10.35848/1347-4065/ac95e6
29 N. Wantana, E. Kaewnuam, Y. Tariwong, N. D. Quang, P. Pakawanit, C. Phoovasawat, N. Vittayakorn, S. Kothan, H. J. Kim, and J. Kaewkhao: Jpn. J. Appl. Phys. **62** (2023) 010602. https://doi.org/10.35848/1347-4065/ac9876
30 D. Shiratori, H. Fukushima, D. Nakauchi, T. Kato, N. Kawaguchi, and T. Yanagida: Jpn. J. Appl. Phys. **62** (2023) 010608. https://doi.org/10.35848/1347-4065/ac90a4
31 H. Masai and T. Yanagida: Jpn. J. Appl. Phys. **62** (2023) 010606. https://doi.org/10.35848/1347-4065/ac91b8
32 K. Shinohara, M. J. F. Empizo, M. Cadatal-Raduban, K. Yamanoi, T. Shimizu, M. Yoshimura, N. Sarukura, and T. Murata: Jpn. J. Appl. Phys. **62** (2023) 010612. https://doi.org/10.35848/1347-4065/aca0d4
33 N. Kawaguchi, K. Watanabe, D. Shiratori, T. Kato, D. Nakauchi, and T. Yanagida: Sens. Mater. **35** (2023) 499. https://doi.org/10.18494/SAM4136
34 Y. Takebuchi, D. Shiratori, T. Kato, D. Nakauchi, N. Kawaguchi, and T. Yanagida: Sens. Mater. **35** (2023) 507. https://doi.org/10.18494/SAM4142
35 H. Kimura, T. Fujiwara, M. Tanaka, T. Kato, D. Nakauchi, N. Kawaguchi, and T. Yanagida: Sens. Mater. **35** (2023) 513. https://doi.org/10.18494/SAM4146
36 H. Kimura, T. Kato, D. Nakauchi, N. Kawaguchi, and T. Yanagida: Sens. Mater. **34** (2022) 691. https://doi.org/10.18494/SAM3687

37 N. Kawaguchi, D. Nakauchi, T. Kato, Y. Futami, and T. Yanagida: Sens. Mater. **34** (2022) 725. https://doi.org/10.18494/SAM3705
38 M. Koshimizu: Jpn. J. Appl. Phys. **62** (2023) 010503. https://doi.org/10.35848/1347-4065/ac94fe
39 R. Nagaoka1, N. Kawano, Y. Takebuchi, H. Fukushima, T. Kato, D. Nakauchi, and T. Yanagida: Jpn. J. Appl. Phys. **62** (2023) 010601. https://doi.org/10.35848/1347-4065/ac943d
40 T. Suto, N. Kawano, K. Okazaki, Y. Takebuchi, H. Fukushima, T. Kato, D. Nakauchi, and T. Yanagida: Jpn. J. Appl. Phys. **62** (2023) 010610. https://doi.org/10.35848/1347-4065/ac8f02
41 K. Okazaki, D. Onoda, D. Nakauchi, N. Kawano, H. Fukushima, T. Kato, N. Kawaguchi, and T. Yanagida: Sens. Mater. **34** (2022) 575. https://doi.org/10.18494/SAM3678
42 D. Onoda, M. Akatsuka, N. Kawano, T. Kato, D. Nakauchi, N. Kawaguchi, and T. Yanagida: Sens. Mater. **34** (2022) 585. https://doi.org/10.18494/SAM3679
43 W. R. Rapoport and C. P. Khattak: Appl. Opt. **27** (1988) 2677. https://doi.org/10.1364/AO.27.002677
44 K. Kniec and L. Marciniak: Sens. Actuators B **264** (2018) 382. https://doi.org/10.1016/j.snb.2018.02.189
45 M. F. Bulanyi, Y. A. Gulevskii, and B. A. Polezhaev: Inorg. Mater. **36** (2000) 997. https://doi.org/10.1007/BF02757974
46 Y. Takada, K. Yamamoto, A. Kinomura, T. Saito, N. Ichinose, A. Okada, T. Wakasugi, and K. Kadono: AIP Adv. **11** (2021) 035208. https://doi.org/10.1063/5.0044309
47 B. V. Padlyak, I. I. Kindrat, Y. O. Kulyk, Y. S. Hordieiev, V. I. Goleus, and R. Lisiecki: Mater. Res. Bull. **158** (2023) 112071.
48 T. Yanagida, K. Kamada, Y. Fujimoto, H. Yagi, and T. Yanagitani: Opt. Mater. **35** (2013) 2480. https://doi.org/10.1016/j.optmat.2013.07.002
49 T. Yanagida, Y. Fujimoto, T. Ito, K. Uchiyama, and K. Mori: Appl. Phys. Exp. **7** (2014) 062401. https://doi.org/10.7567/APEX.7.062401
50 W. C. Wong, D. S. McClure, S. A. Basun, and M. R. Kokta: Phys. Rev. B **51** (1995) 5682. https://doi.org/10.1103/PhysRevB.51.5682
51 Y. Takebuchi, H. Fukushima, T. Kato, D. Nakauchi, N. Kawaguchi, and T. Yanagida: Radiat. Phys. Chem. **177** (2020) 109163. https://doi.org/10.1016/j.radphyschem.2020.109163
52 P. S. Page, B. S. Dhabekar, B. C. Bhatt, A. R. Dhoble, and S. V. Godbole: J. Lumin. **130** (2010) 882. https://doi.org/10.1016/j.jlumin.2009.12.029
53 S. García-Revilla, F. Rodríguez, R. Valiente, and M. Pollnau: J. Phys.: Condens. Matter **14** (2002) 447. https://doi.org/10.1088/0953-8984/14/3/313
54 F. Bantien, P. Albers, and G. Huber: J. Lumin. **36** (1987) 363. https://doi.org/10.1016/0022-2313(87)90153-0
55 J. D. Hewitt, T. M. Spinka, A. A. Senin, and J. G. Eden: Appl. Phys. Lett. **99** (2011) 031101. https://doi.org/10.1063/1.3614001
56 P. C. Ricci, A. Casu, and A. Anneda: J. Phys. Chem. A **113** (2009) 13901. https://doi.org/10.1021/jp906864a
57 K. Kniec, M. Tikhomirov, B. Pozniak, K. Ledwa and L. Marciniak: Nanomaterials **10** (2020) 189. https://doi.org/10.3390/nano10020189
58 S. N. Oguguaa, O. M. Ntwaeaborwab, and H. C. Swarta: Bol. Soc. Esp. Ceram. Vidrio **60** (2021) 147. https://doi.org/10.1016/j.bsecv.2020.02.005
59 T. Hasegawa, Y. Abe, A. Koizumi, T. Ueda, K. Toda, and M. Sato: Inorg. Chem. **57** (2018) 857. https://doi.org/10.1021/acs.inorgchem.7b02820
60 G. Blasse and J. Hop: J. Solid State Chem. **27** (1979) 423. https://doi.org/10.1016/0022-4596(79)90184-1
61 A. Majewski-Napierkowski, V. Gorbenko, T. Zorenko, S. Witkiewicz-Łukaszek and Y. Zorenko: Crystals **13** (2023) 1481. https://doi.org/10.3390/cryst13101481
62 Y. Fujimoto, T. Yanagida, H. Yagi, T. Yanagidani, and V. Chani: Opt. Mater. **36** (2014) 1926. https://doi.org/10.1016/j.optmat.2014.06.019
63 S. M. Reda, C. R. Varney, and F. A. Selim: Results Phys. **2** (2012) 123. https://doi.org/10.1016/j.rinp.2012.09.007